Chemical Engineering & Processing: Process Intensification 179 (2022) 109052

Contents lists available at ScienceDirect

Chemical Engineering and Processing - Process Intensification

journal homepage: www.elsevier.com/locate/cep

Process modelling and feasibility study of sorption-enhanced methanol synthesis

Harri Nieminen [a,*], Pavel Maksimov [a], Arto Laari [a], Virpi Väisänen [b], Ari Vuokila [b], Mika Huuhtanen [b], Tuomas Koiranen [a]

[a] LUT university, LUT School of Engineering Science, P.O. Box 20, FI-53851 Lappeenranta, Finland
[b] University of Oulu, Environmental and Chemical Engineering, P.O. Box 4300, FI-90014 University of Oulu, Finland

ARTICLE INFO

Keywords:
CO_2 hydrogenation
Methanol synthesis
Power-to-X
Sorption-enhanced
Techno-economic
Process modelling

ABSTRACT

A sorption-enhanced process for hydrogenation of CO_2 to methanol was designed and investigated by mathematical modelling and techno-economic analysis. The modelling methodology combined dynamic modelling of the cyclic reactor operation with pseudo-steady state modelling of the overall process. With continuous adsorption of water in the sorption-enhanced process, highly pure methanol (>99%) was produced without downstream distillation. The dynamic reactor cycle was designed and optimized to maximize the methanol production rate. The cycle and the process were modelled in two reactor configurations: adiabatic and isothermal. Under the default cost assumptions for the raw materials (CO_2 50 €/t, hydrogen 3000 €/t) the adiabatic configuration was found more competitive in terms of the overall methanol production cost, at 1085 €/t compared to 1255 €/t for the isothermal case. The cost estimate for the adiabatic case was found comparable to a reference process representing conventional CO_2 hydrogenation to methanol (1089 €/t). In addition to the methanol process, the developed modeling method has potential in the design of other sorption-enhanced processes.

1. Introduction

Production of synthetic fuels and chemical products from captured carbon dioxide (CO_2) using renewable energy as the primary energy source has been suggested as a pathway to reduce CO_2 emissions in the energy and chemical sectors [1]. Utilizing hydrogen generated by water electrolysis in such conversions would facilitate the storage of variable and intermittent renewable electricity into storable and transportable carbon-containing fuels [2,3]. At the same time, this would allow the use of CO_2 as a carbon source and replacement for fossil feedstock in the chemical industries [4,5].

Of such synthetic fuels and chemicals, methanol constitutes a particularly interesting product as solvent, and especially due to its versatility and multiple potential end-uses in both the energy and chemical sectors [6]. Via various successive conversion steps, practically any of the major fuel or chemical products currently originating from fossil feedstock could be reached via methanol as a platform chemical [7]. Global annual methanol production is around 85 Mt which is slightly lower than the largest bulk chemical, ethene (>100 Mt) [8]. Major industrial chemicals obtained via methanol include acetic acid, formaldehyde, dimethyl carbonate, methyl tert-butyl ether, and several methyl based organic derivatives. For fuel uses, methanol can directly be blended in gasoline, or converted into hydrocarbon fuels via the methanol-to-gasoline process, for instance. In addition, methanol can be converted to olefins (ethylene, propylene) via the methanol-to-olefins conversion.

Methanol synthesis via hydrogenation of CO (Eq. (1)) and/or CO_2 (Eq. (2)) on established copper/zinc oxide (Cu/ZnO) catalysts usually takes place in a temperature range of 200-300°C and in pressures between 50 and 100 bar [9,10]. The water gas shift reaction (Eq. (3)), also activated by the Cu/ZnO catalyst, is a key side reaction and can proceed in either direction depending on the feed gas composition and reaction conditions. In CO_2-based methanol synthesis, this reaction generally proceeds in the reverse direction, and is referred to as reverse water gas shift (RWGS).

$$CO_2 + 3\ H_2 \rightleftharpoons CH_3OH + H_2O \qquad \Delta H = -49.8\ \text{kJ/mol.} \tag{1}$$

$$CO + 2\ H_2 \rightleftharpoons CH_3OH \qquad \Delta H = -91.0\ \text{kJ/mol.} \tag{2}$$

* Corresponding author.
E-mail address: harri.nieminen@lut.fi (H. Nieminen).

https://doi.org/10.1016/j.cep.2022.109052
Received 20 April 2022; Received in revised form 1 July 2022; Accepted 9 July 2022
Available online 16 July 2022

Nomenclature

Symbols

C:	Capital cost element
F:	Capital cost correction factor

Subscripts

con:	contingency
e:	installed equipment cost
eng:	engineering
l:	location
ci:	cost index

Abbreviations

CEPCI:	Chemical Engineering Plant Cost Index
GHSV:	gas hourly space velocity
ISBL:	inside battery limits
OSBL:	outside battery limits
A:	pressure swing adsorption
RWGS:	reverse water-gas shift
SE:	sorption-enhanced
VLE	vapor-liquid equilibrium

$$CO + H_2O \rightleftharpoons CO_2 + H_2 \qquad \Delta H = -41.2\ \text{kJ/mol.} \tag{3}$$

Compared to conventional (synthesis gas-based) methanol synthesis, major challenges in CO_2-based methanol synthesis are the unfavorable chemical equilibrium leading to decreased per-pass conversion, and the increased formation of water as by-product. Excessive water concentrations have been shown to inhibit methanol synthesis on Cu/ZnO catalysts via the mechanism of competitive adsorption [11].

Various approaches have been pursued in order to improve the per-pass conversion in CO_2 hydrogenation to methanol. As methanol formation is faved by lower temperatures and higher pressures, many of these approaches have accordingly relied on extending the reaction conditions from the conventional ranges of temperature and pressure.or instance, up to full CO_2 conversion has been demonstrated at very high pressures [12,13] and inovel reactor configurations with internal product condensation [14]. Reduced reaction temperatures can also be accessed in three-phase reactions utilizing co-catalytic solvents, such as alcohols, capable of modifying the reaction mechanism [15].

Another approach to improve the conversion is the selective removal of reaction products during reaction. For example, water can be removed from the reaction mixture by permeation from membrane reactors [16]. Of primary interest in this study is the removal of water by selective adsorption. Promising examples of such sorption-enhanced reactions include methanol and dimethyl ether synthesis [17], the water-gas shift [18], and CO_2 methanation [19]. Thermodynamic modelling of methanol synthesis suggests that complete removal of water directly from the reactor can significantly increase the CO_2 conversion under typical reaction conditions [20]. Similar results have been obtained using more detailed dynamic reactor models capable of predicting the saturation of adsorbent with water over the reaction cycle [21,22]. Beyond the improved chemical equilibrium, another advantage in sorption-enhanced methanol synthesis is simplified product separation, as adsorption of water results in increased purity of crude methanol removed from the reactor.

In our previous study [23], an experimentally validated dynamic model was developed for the investigation of the sorption-enhanced methanol synthesis process. The novelty of this model was in the re-adjustment of established kinetic parameters developed for steady-state methanol synthesis to take into account the kinetic effects of water sorption, leading to improved prediction of the dynamic sorption-enhanced reaction. The model was successfully used in the development and optimization of reaction and adsorbent regeneration cycles for this process.

The present study extends this work by developing and modelling a full process configuration for CO_2-based, sorption-enhanced methanol synthesis. The modelling approach combines dynamic reactor modelling with pseudo-steady state modelling of the overall process for calculation of the dynamic mass and energy balances. The developed method was found effective for analysis of the relatively complex, dynamic process, and could be utilized for other sorption-enhanced processes, or similar dynamically operated processes in general. Process design and production costs have previously been reported for sorption-enhanced dimethyl ether synthesis [24], but not for sorption-enhanced methanol synthesis, to the authors' knowledge. Therefore, the resulting methanol production costs were estimated in order to assess the potential competitiveness of this process compared to conventional CO_2 hydrogenation.

2. Methodology

The results of this study were obtained by combining dynamic modelling of the reaction cycle (MATLAB R2021a) and steady-state modelling of the overall process (Aspen Plus V11).

2.1. Process configuration and scale

The sorption-enhanced process is developed to produce methanol from CO_2 and hydrogen. It is assumed that CO_2 is captured from various point sources, such as power generation plants or industrial processes. Hydrogen would be sourced from water electrolysis powered by renewable electricity sources, such as wind or solar. The process, as designed, is intended for relatively small-scale and distributed production of methanol with such plants possibly located at the electricity source. The considered methanol production rate is in the range of 11–16 kt of methanol per year (2.4–3.7 t/h of CO_2 and 0.3–0.4 t/h of H_2 input), depending on the process configuration. For reference, 18–24 MW of electrolyzer capacity would be required to generate the hydrogen input, assuming specific electricity consumption of 60 kWh/kg, representing a relatively small scale wind power installation.

The overall sorption-enhanced process is illustrated in Fig. 1. The dynamic process is based on the continuous cycle consisting of reaction-adsorption and adsorbent regeneration steps. The purpose and implementation of each step, the overall cycle design and timing, and the process modelling methodology are discussed in Section 2.2.

The process is developed in two distinct configurations, employing either adiabatic packed bed or isothermal boiling-water reactors for methanol synthesis. Besides the reactor arrangement, both process configurations (termed 'adiabatic' and 'isothermal') are identical. The process flow diagrams for the reaction and adsorbent regeneration steps are presented in Figs. 2 and 3, respectively. The flowsheets consist of parallel reactors required for continuous operation of the cyclic sorption-enhanced process. Product separation is carried out by condensation of methanol and water and separation in successive high- and low-pressure gas-liquid separators. Separated gases are combusted in a waste heat boiler to provide heat required during the process cycle.

Regeneration of water-saturated adsorbent within the reactors is carried out under a purge gas (CO_2) flow at reduced pressure. The following scheme is suggested to remove the desorbed water from the purge gas. The outlet gas is first cooled to 10°C (using chilled water or other coolant) to condense most of the water, which is then separated from the gases. The remaining gases are further dried in an adsorption-based drying unit and recycled to the reactor. The details of the adsorptive drying unit are outside the scope of this work. In practice, this step could be carried out by a continuous temperature-swing adsorption unit with a minimum of two columns.

In contrast to conventional methanol synthesis processes, we suggest a separation scheme completely omitting distillation. Facilitated by the adsorption of water in the reactor, crude methanol at high purity can be

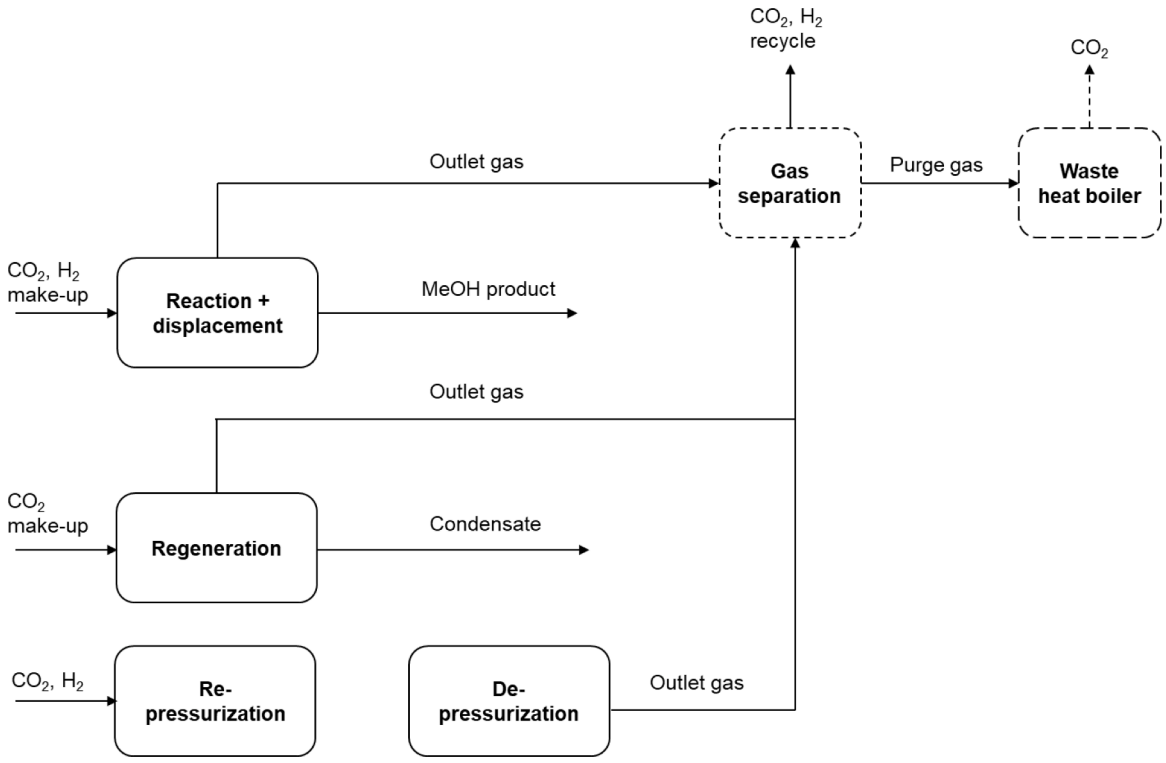

Fig. 1. Block diagram of the overall sorption-enhanced methanol synthesis process with involved process steps and inlet and outlet streams. During re- and depressurization, accumulation (no outlet flow) and discharge (no inlet flow) of material takes place.

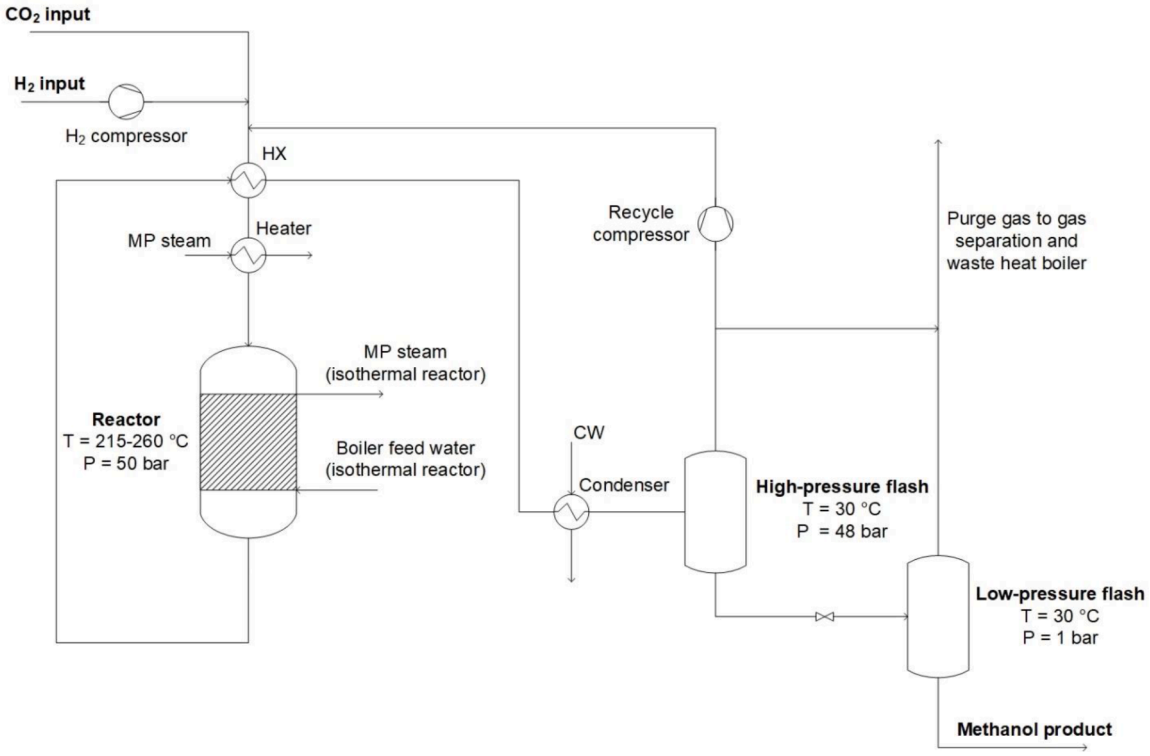

Fig. 2. Flow diagram of the sorption-enhanced methanol synthesis process during the reaction and displacement steps. MP = medium pressure, 200-300°C.

produced by condensation and removal of unreacted gases. Here, we aim for a crude methanol purity of 99.0 w-%. As such, the methanol product does not directly fulfil the requirements for chemical grade methanol but could be directly utilized in fuel blends or as feedstock for further conversion processes. Example of the latter would be the conversion of methanol to hydrocarbon fuels or olefins on zeolite catalysts [7]. Methanol blended with up to 15% water has been suggested as a fuel for internal combustion engines [25]. Use of methanol-water

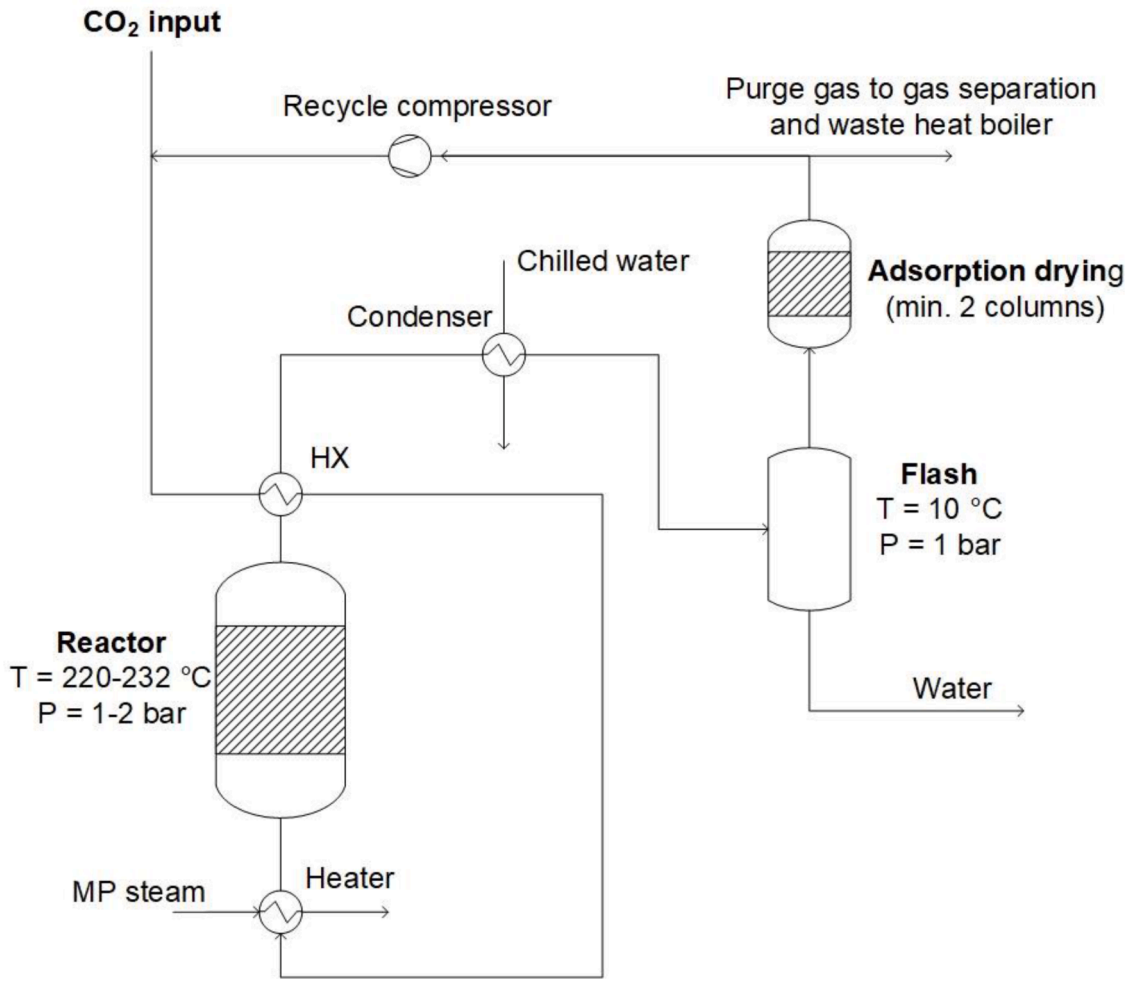

Fig. 3. Flow diagram of the sorption-enhanced methanol synthesis process during the adsorbent regeneration step.

mixtures in direct methanol fuel cells could also be feasible [26]. It is highlighted that the sorption-enhanced process could be adapted and optimized for any methanol concentration required by the considered application.

The reactor/separation loops during the reaction and adsorbent regeneration steps were designed prioritizing simplicity. The number of equipment was kept to a minimum, and heat integration was only considered at the most obvious locations (reactor outlet-inlet). When possible, condensation temperatures at flash separators were set to the minimum temperature that can be handled by cooling water, assumed at 30°C. Lower temperatures requiring chilled water or similar coolant were employed during regeneration to ensure sufficient condensation of

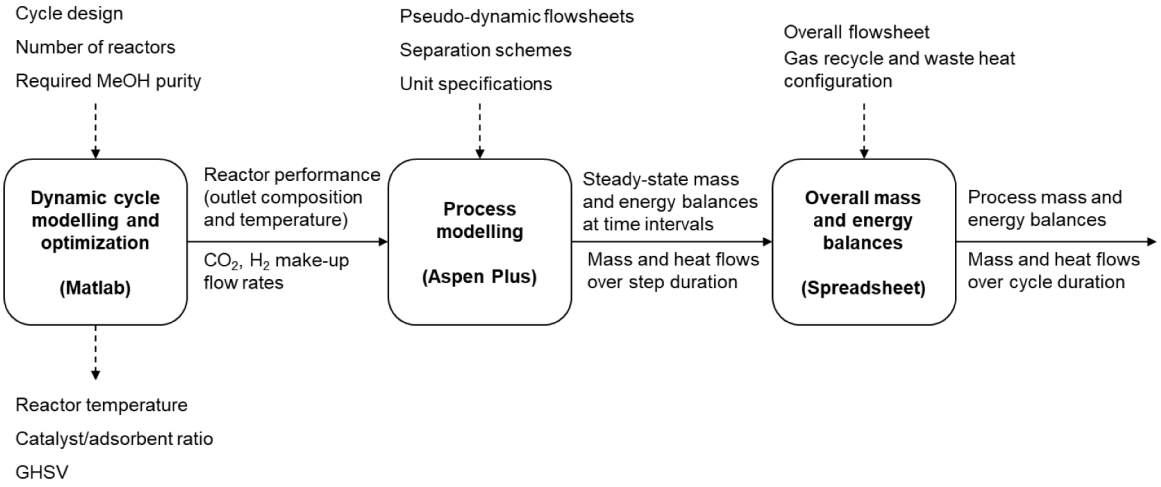

Fig. 4. Illustration of the modelling approach employed in this study. Solid lines represent model input and outputs, dashed lines represent model parameters. GHSV: gas hourly space velocity.

water. Temperature approaches in heat exchangers were set according to common heuristics based on phases present. More details on equipment design bases are given in the Supplementary material (Table SIV–SV).

2.1.1. Modelling approach

For calculation of the mass and energy balances of the sorption-enhanced methanol synthesis process, a combined approach utilizing both dynamic reactor modelling and pseudo-steady state modelling of the overall process was adopted. The overall modelling approach is illustrated in Fig. 4. The dynamic reactor model was utilized for the development of the reactor cycles and prediction of the reactor performance. The results from this model were then extracted as input data to the overall process model developed in Aspen Plus (V11). In order to investigate the performance of the cyclic process by means of steady-state process modelling, a pseudo-dynamic approach was used: data was extracted from the results of dynamic model at selected interval during the duration of the reaction cycle. This method is explained in Section 2.2.2.

2.1.2. Reactor cycle modelling

Sorption-enhanced synthesis is an inherently dynamic process as it involves both reaction and adsorption phenomena. Because of the limited sorption capacity, the adsorbent should be periodically regenerated to desorb the adsorbed water. Since the desorption rate is inversely proportional to the water partial pressure, reducing the reactor pressure improves regeneration. Therefore, a typical pressure swing adsorption (PSA) cycle is the most time-efficient regeneration scheme for the considered process. A detailed description of the complete PSA cycle consisting of pressurization, reaction, depressurization and regeneration steps was described previously [27]. Considering the axial profile of the loading of water on adsorbent in the reactor at the end of the reaction step, the flow of the gases during the depressurization and regeneration steps is arranged in the direction opposite to the flow of the gases during the pressurization and reaction steps.

As the reactor outlet during the depressurization step contains considerable amount of desorbed water, collecting this product might be impractical since it may decrease methanol product purity. Therefore, an additional displacement step is implemented to enable convenient collection of the methanol still present in the reactor after the reaction step is complete under the same pressure and temperature. This step involves feeding pure purge gas (CO_2) in the same direction as during the reaction step thus pushing the methanol product out of the reactor. Once the displacement step is complete and all the methanol product is removed from the reactor, the depressurization and regeneration steps are performed without any alterations.

A previously developed and validated dynamic reactor model [28] was used to estimate the performance of the sorption-enhanced reactor for methanol synthesis [28]. The model is one-dimensional, pseudo--homogeneous, non-isobaric and non-isothermal. The bed is considered to consist of a homogeneous mixture of the methanol synthesis catalyst and 3Å molecular sieve. Since there is no experimental or other evidence that catalyst activity or adsorbent capacity decreases during the operation, any changes in catalyst or adsorbent behavior are neglected in the models. The complete PSA cycle was modelled by consecutively simulating the separate steps of the cycle with the reactor model with adjusted boundary and initial conditions. To evaluate the cyclic steady state performance, the system was simulated for 30 consecutive PSA cycles.

The kinetics of the methanol synthesis reactions were described with the kinetic interpretation proposed by Graaf et al. [29,30] as their model was experimentally validated to accurately estimate methanol production rate on the employed catalyst [31]. Accounting for the in-situ removal of water, the readjusted values of the kinetic and adsorption constants were taken from our previous work [32] along with the parameters of the Langmuir adsorption isotherm used to evaluate the adsorbent equilibrium loading under the sorption-enhanced methanol synthesis conditions. While all the details of the dynamic reactor model are provided in our previous works [23,32,27,28], governing equations forming the basis of the model are also described in the Supplementary information.

The flash separation units were modelled by solving the Rachford-Rice equation [33] with the phi-phi method [34] employed for calculation of the vapor-liquid equilibrium. The values of fugacity coefficients and compressibility factors were evaluated with the Soave-Redlich-Kwong equation of state [35]. This thermodynamic model has been shown [30,36] to accurately predict the chemical equilibrium under methanol synthesis conditions [30,36], and was also successfully used to describe our own experimental findings on sorption-enhanced methanol synthesis [32].

It is assumed that the residence time of 5 minutes is sufficient to achieve vapor-liquid equilibrium in the flash separation units. Complete recirculation of the vapor phase from the high-pressure flash separation unit is considered, and the constant GHSV in the reactor is maintained by adjusting the make-up flowrate of the fresh H_2/CO_2 mixture. A detailed description of the methodology employed for the recirculation modeling accounting for the residence time in the flash drum is provided in our previous work [23] along with the governing equations and boundary conditions forming the basis of the reactor model.

Based on the multi-objective optimization results [23], the process parameters and the overall cycle design were adjusted to comply with the target purity of 99.0 w-% for the blend methanol product after achieving the cyclic steady state. Particularly, reactor temperature, catalyst/adsorbent ratio, and GSHV for reaction and regeneration steps were varied to maximize the specific methanol production rate keeping the required product purity. As a constraint, the total reactor volume was maintained constant in both reactor configurations. This was done to provide a consistent analysis of the differing characteristics and performance of the two configurations.

The reactor pressure during the reaction step was fixed at 50 bar, as this pressure is considered practical for industrial scale methanol synthesis [10]. In this regard, taking account of the data reported by Boon et al. [18] on the dynamic operation of sorption-enhanced reactors, the duration of the pressurization and depressurization steps duration was set as 5 minutes. In light of this and bearing in mind the previously determined optimal durations of the reaction and regeneration steps [23], the 3-reactor configuration is considered to ensure continuous production of methanol. Hence, the purge gas inlet flowrate was adjusted to ensure sufficient adsorbent regeneration within 10 minutes of the regeneration step, while 8 and 2 minutes were set for the reaction and displacement step, respectively. The determined cycle design is presented in Fig. 5. This cycle configuration provides an opportunity to achieve maximum specific methanol production rate while maintaining the required product purity (99 w-%) and abiding by the practical time constraints (matching of steps between parallel reactors to facilitate continuous methanol production). The resulting reactor sizing and configuration are discussed in Section 3.1.

Pure CO_2 is used as the purge gas during the displacement and regeneration steps to ensure the possibility of efficient recirculation. More specifically, if pure CO_2 is used as the reactor feed during the displacement step, the reactor outlet stream can be collected and reused in the process as it would consist predominantly of CO_2 following condensation of methanol and water. Similarly, utilizing CO_2 during the regeneration step is practical as this way no unnecessary mixing of the gases occurs.

2.1.3. Process modelling

The dynamic reactor model (MATLAB) was used to predict the performance of the adiabatic and isothermal reactor loops including gas circulation. The results were then used as inputs to set up the corresponding models of the overall process (including product separation, heat transfer, and compression) in Aspen Plus. Separate simulation

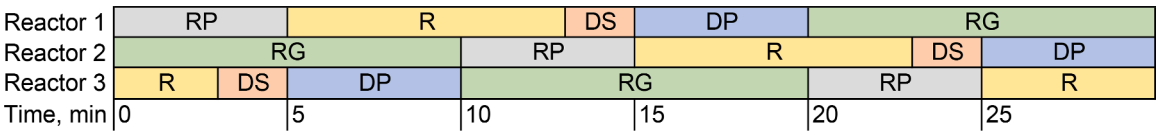

Fig. 5. Cycle design and timing for continuous sorption-enhanced methanol synthesis based on three parallel reactors. The same cycle is used for both adiabatic and isothermal reactor configurations. R: reaction, DS: displacement, DP: depressurization, RG: regeneration, RP: repressurization.

flowsheets were developed for the reaction and regeneration steps. The displacement step was also modelled using the reaction model, as the flow connections are identical. Each flowsheet follows the basic design illustrated in Figs. 2 and 3. The corresponding simulation flowsheets and details on the model implementation are given in the Supplementary information. The Aspen Plus models are based on the Soave-Redlich-Kwong equation of state. It should be noted that activity coefficient-based models are often preferred to model methanol-water distillation [37]. However, in the suggested process, distillation is not required due to near-complete separation of water by adsorption. In general, this equation of state is commonly used for process modelling studies involving similar components and process conditions to the present case [38].

Table 1 details the required input data to the reaction (displacement) and regeneration step models. All data is collected from the results of the dynamic cycle model, at the time resolution of one minute. The steady-state Aspen Plus models are run correspondingly at the same one-minute resolution using the results of the dynamic model as inputs. As a result, the dynamic mass and energy balances of the overall process are obtained over the reaction cycle.

In the reaction and displacement model, the reactor is not included as a block in the process model. Instead, component flow rates at the reactor outlet (pseudo-) stream are directly set equal to the reactor outlet stream from the dynamic model. By leaving out the actual reactor from the model, the total flow rate and composition at reactor inlet and outlet are decoupled, allowing the accurate replication of dynamic reactor performance in the steady-state model. In the isothermal case, the reactor heat duty over the cycle is directly extracted from the results of the dynamic model. The reactor outlet temperature is adjusted to match the dynamic model results using a Heater block. It should be noted that this block does not represent actual process equipment but is added to simulate the overall performance of the reactor. The parameters and assumptions for setting up the reaction and displacement model are given in Table 2.

In the regeneration model, the make-up CO_2 flow rate is adjusted by a design specification, setting the CO_2 flow rate at reactor inlet equal to the flow rate in the dynamic model. As opposed to the dynamic model, the purge gas is not pure CO_2 as it also contains minor fractions of H_2 and CO that are removed from the reactor and recycled. Based on tests using the dynamic cycle model (results not shown here), the composition of the purge gas does not affect the regeneration performance if the moisture content is maintained low. The flow rates of water and other components removed from the reactor during regeneration are adjusted by a separate inlet pseudo-stream, which does not represent an actual stream in the process. Similar to the reaction step model, the reactor outlet temperature is adjusted by a Heater block, which again does not represent an actual process unit. The gas drying step is modelled as a simple separator, where 99% of water is assumed to be removed. The parameters and assumptions for setting up the regeneration model are given in Table 3.

It should be noted that the flow rates obtained from the Aspen Plus models can deviate from those predicted by the dynamic model at the same point in time over the reaction cycle. There are two key reasons for these deviations. First, unlike the dynamic model, the steady-state process model does not take into account the time delay caused by the residence time of components within the process units. In contrast, the outlet flow rates at each time point are calculated based on the instantaneous inlet flow rates, leading to a time shift equal to the actual

Table 1
Results from the dynamic cycle model used as input in the steady-state process models.

Reaction and displacement	Regeneration
CO_2 make-up flow rate, mol/s	CO_2 purge flow rate at reactor inlet, mol/s
Hydrogen make-up flow rate, mol/s	Component flow rates at reactor outlet, mol/s
Component flow rates at reactor outlet, mol/s	Reactor outlet temperature,°C
Reactor outlet temperature,°C	

Table 2
Modelling parameters and assumptions in the Aspen Plus model for the reaction and displacement steps, and the corresponding values for the adiabatic and isothermal reactor configurations.

Parameter	Adiabatic	Isothermal	Basis
Hydrogen inlet pressure, bar	30.0		From electrolyzer or storage
Hydrogen inlet temperature,°C	25.0		Ambient
CO_2 inlet pressure, bar	50.0		From capture process, transport or storage
CO_2 inlet temperature,°C	25.0		Ambient
Reactor inlet temperature,°C	215.9	220.0	Reaction cycle optimization
Temperature approach in pre-heater,°C	30.0		Gas-gas exchanger heuristic
Condenser and flash temperature,°C	30.0		Cooling water utility
Pressure drop over reactor loop, bar	2.0		Approximated using Darcy's law (reactor only)
Recycle gas purge fraction (reaction)	1%		Heuristic
Recycle gas purge fraction (displacement)	100%		Reactor is purged with pure CO_2

Table 3
Modelling parameters and assumptions in the Aspen Plus model for the regeneration step. The value of each parameter is equal for the adiabatic and isothermal reactor configurations.

Parameter	Adiabatic and isothermal	Basis
CO_2 inlet pressure, bar	2.5	Based on estimated pressure drop
CO_2 inlet temperature,°C	25.0	Ambient
Reactor inlet temperature,°C	220.0	Reaction cycle optimization
Temperature approach in pre-heater,°C	30.0	Gas-gas exchanger heuristic
Condenser and flash temperature,°C	10.0	Adjusted to maximize water condensation (chilled water or other coolant)
Fraction of water removed in drying (adsorption)	99%	
Pressure drop over reactor loop, bar	1.5	Approximated using Darcy's law (reactor only)
Recycle gas purge rate	1%	Heuristic

residence time throughout the overall process. This time shift is in the order of 5 min for the reaction and displacement steps.

Second, deviation can be caused by the predicted separation and recycle of unreacted gases in the dynamic and steady-state models. While both types of models utilize the Soave-Redlich-Kwong equation of state to predict the vapor-liquid equilibrium (VLE), there are necessarily differences between the MATLAB calculations and the algorithms contained in Aspen Plus for modelling of the VLE and the flash separation units. In addition, the steady-state models include the fractional purge of circulated gases, which is not included in the dynamic model.

2.1.4. Re- and depressurization flow rates

While the re- and depressurization steps were included in the overall dynamic model of the reaction cycle (Section 2.2.1), the time-dependent input and output flow rates during these steps were not calculated in detail in order to simplify the model. Instead, the total cumulative component flow rates during these steps were collected as results from the model. Based on the cumulative flows, the average flow rates of each component over the re- and depressurization steps were then calculated.

This approach led to a problem with the overall process mass balance when compiling the results of the process modelling. As described above (Section 2.2.2), the approach of using steady-state process models to calculate the process mass balances at successive points in time is not able to take into account the residence time effect of the dynamic model. Such steady-state models were not used for the re- and depressurization steps. Instead, results of the dynamic model were directly used, leading to inconsistencies when compiling the cycle mass balances. The observed deviation could be corrected by manual adjustment of the outlet flow rates during the depressurization step. The corrected flow rates obtained by this method are included in the final mass balances presented in this study (Section 3.2).

2.1.5. Gas separation and waste heat combustion

For efficient operation of the sorption-enhanced methanol synthesis process, the gases purged from the process during the various operating steps have to be utilized. In this study, we suggest a simplified scheme consisting of separating and recycling both CO_2 and H_2 that are removed during the reaction, displacement, regeneration and depressurization steps, and combusting the remaining purge gases to provide process heat, as illustrated in Fig. 1. Thus, an additional gas separation stage is included in the overall mass balance calculations. This separation is assumed to remove 90% of CO_2 and H_2 contained in the outlet gas streams, with both separated at 100% purity. Following gas separation, the remaining gases are routed to a waste heat boiler, where steam is generated to provide utility heat required during the different process steps. The amount of steam generated is calculated based on the lower heating value of the components, assuming 85% efficiency.

The separated CO_2 and H_2 are recycled as inputs to the process steps, decreasing the amount of make-up gases required. As a further simplification, all variation in the temperature, pressure, composition and flow rate of each purge stream from the process steps over the cycle duration are neglected. Details of this separation are outside the scope of this study, but separation of CO_2 and H_2 could be feasibly carried out using various methods that are utilized in hydrogen or synthesis gas production, for instance by physical or chemical scrubbing of CO_2, cryogenic or membrane separation, or pressure-swing adsorption [39].

It should be noted that separation of CO_2 and H_2 at high purity might not be necessary at all. As the components in the purge gas are already present within the reactor loop, the outlet gas could feasibly be directly re-circulated as inputs to the various process steps. This is especially the case for the regeneration and depressurization outlet streams, which essentially consist of only CO_2 (Supplementary information, Table SVI). Only minor separation or purification steps might be required in order to adjust the recycle gas composition and to remove contaminants or minor by-products. In this study, the direct re-circulation of the outlet gases is not investigated as this would require a computationally intensive iteration loop over the whole process for modelling of the cycle at variable make-up gas composition.

3. Cost estimation

To assess the economic potential of the suggested sorption-enhanced methanol synthesis process, the resulting methanol production costs were estimated. Costs were estimated for both the adiabatic and isothermal reactor configurations. Equipment costs were estimated based on the Aspen Economic Evaluation functionality in Aspen Plus. The total capital costs and fixed operating costs were then estimated using the factorial methodology [35,36] based on the equipment cost estimates. Variable operating costs were estimated based on feedstock and utility input costs. The main assumptions for the economic analysis are presented in Table 4. Details on the cost estimation procedure are given in the Supplementary information.

4. Results and discussion

The results of this study consist of the optimized cycle design and reactor sizing based on the results of the dynamic cycle model, the mass and energy balances of the overall process calculated using the steady-state process models, and production cost estimates. To highlight the characteristics of the sorption-enhanced processes, key results are compared to a reference process representing more conventional CO_2 hydrogenation, as investigated in our previous study [40].

4.1. Cycle design and optimization

Table 5 presents the optimized reactor configuration and sizing for the adiabatic and isothermal cases. Reactor sizing is based on setting the overall bed volume equal in the two cases. For the adiabatic and isothermal cases, the gas hourly space velocity during each process step is optimized using the dynamic cycle model. As described in Section 2.2.1, the target for optimization was to maximize the methanol production rate over the cycle, while maintaining 99 w-% purity in the methanol product. Note that catalyst mass fraction refers to the catalyst/adsorbent ratio within the mixed reactor bed. The total mass of adsorbent is increased by the additional adsorbent-only guard layer located at the reactor outlet, occupying 10% of the total bed volume [23].

In comparison of the adiabatic and isothermal cases, of note is the higher space velocity during reaction and regeneration in the isothermal case. In the isothermal case, the reactor temperature during the reaction step is maintained lower which facilitates higher adsorbent water capacity. Thus, more methanol can be produced prior to breakthrough of water. Setting the reaction time equal for both configurations, this means that reactants can be fed and converted at a higher rate in the isothermal case. Correspondingly, as more water is adsorbed during reaction, the rate of water removed during the regeneration step has to be higher in the isothermal case. This requires a higher purge gas flow rate in order to maintain an equal regeneration duration and to ensure sufficient adsorbent regeneration.

Here, comparison between the two cases was made by setting the catalyst/adsorbent masses and reactor bed volumes equal. Alternatively, a meaningful comparison could have been made by setting equal inlet flow rates, either averaged over the cycle, or during the reaction step.

Table 4
Main economic assumptions for estimation of production costs.

Plant lifetime	20 years
Operating hours	8000 h/year
Discount/interest rate	8%
Hydrogen cost	3000 €/t
CO_2 cost	50 /t

Table 5
Catalyst and adsorbent loading, reactor sizing, and gas-hourly space velocity (GSHV) for each individual reactor in the adiabatic and isothermal reactor configurations.

Catalyst/adsorbent bed	Adiabatic	Isothermal
Catalyst mass per reactor, kg	9 695	9 695
Adsorbent mass per reactor, kg	11 202	11 202
Catalyst mass fraction	0.5	0.5
Guard layer, % of bed volume	10	10
Reactor sizing		
Volume, m^3	25.13	25.13
Length, m	8	7
Inner diameter, m	2	0.035 (tube)
Number of tubes	-	3750
Flow parameters		
GHSV (reaction), h^{-1}	300	520
GHSV (displacement), h^{-1}	380	380
GHSV (regeneration), h^{-1}	1650	2500
Interstitial gas velocity, m/s (reaction)[1]	0.07	0.11
Interstitial gas velocity, m/s (displacement)[1]	0.09	0.08
Interstitial gas velocity, m/s (regeneration)[1]	8.72	11.13

[1] At reactor inlet.

This would have resulted in smaller reactor size in the isothermal case. Qualitatively, the results would not be different, and only the relative flow rates in the isothermal case would be reduced compared to the adiabatic case. The same would be seen in the process energy balances, as compared in Section 4.3. In terms of production costs (Section 4.4), the methanol-rate-specific costs in the isothermal case would be slightly increased as the small economy of scale advantage over the adiabatic case would be removed.

Table 6 summarizes the resulting input molar flow rates of H_2 and CO_2 during the process cycle. During the reaction step, the input flow rates are varied in order to maintain the total feed flow rate, including the recycled gases, constant. The flow rate of recycled gases vary during the dynamic reaction step, as the adsorbent is saturated by water. In the fresh feed (make-up) stream, the molar ratio of H_2 and CO_2 is always fixed at 3:1.

4.2. Process mass balances

The following tables present the component maximum and average mass flow rates, and cumulative mass flows at inlet and outlet streams during different steps over the reaction cycle. The corresponding streams are illustrated in Fig. 1. Inlet streams are presented in Table 7. Outlet streams are presented in Table 8 for the reaction and displacement steps, and in Table 9 for the regeneration and depressurization steps. The composition of the gas outlet streams removed during each step is presented in Table SVI (Supplementary information). The inlet streams refer to the total inputs consisting of make-up and recycled CO_2 and H_2 (see Section 2.2.4).

Table 6
H_2 and CO_2 feed (make-up) molar flow rates during each process step, in the adiabatic and isothermal reactor configuration. The flow rates during the reaction step vary within the range given, but the molar ratio of H_2 and CO_2 remains fixed.

Process step	H_2 feed flow rate, mol/s	CO_2 feed flow rate, mol/s	H_2/CO_2 molar ratio (fixed)
Reaction	28.5–46.7 (adiabatic) 57.7–71.0 (isothermal)	9.5–15.6 (adiabatic) 19.3–23.7 (isothermal)	3:1
Displacement	0	93.5 (adiabatic) 162.9 (isothermal)	0:1
Regeneration	0	514.3 (adiabatic) 783.0 (isothermal)	0:1
Repressurization	38.9 39.1	13.1 (adiabatic) 13.1 (isothermal)	3:1

Table 7
Component maximum, average and cumulative flow rates at process inlet streams over the reaction cycle, in the adiabatic (figures above) and isothermal (figures below) reactor configuration.

Step	Reaction + displacement		Regeneration	Pressurization	
Inlet stream/ component	CO_2	H_2	CO_2	CO_2	H_2
Maximum flow rate, kg/s	14.81 25.80	0.34 0.52	0.82 1.24	2.07 2.08	0.28 0.28
Average flow rate, kg/s	4.51 7.86	0.21 0.37	0.82 1.24	1.04 1.04	0.14 0.14
Cumulative flow per cycle, kg	2257 3928	107 185	411 620	518 520	71 71

Table 8
Component maximum, average and cumulative flow rates at process outlet streams over the reaction and displacement steps, in the adiabatic (figures above) and isothermal (figures below) reactor configuration. Components with minor flows (cumulative <1 kg) are not included.

Step	Reaction + displacement						
Outlet stream	Product			Purge gas			
Component	CO_2	MeOH	Water	CO_2	H_2	CO	MeOH
Maximum flow rate, kg/s	0.01 0.02	1.62 2.60	0.01 0.01	5.61 2.02	0.47 0.59	1.40 0.68	0.09 0.07
Average flow rate, kg/s	0.01 0.02	1.34 2.04	0.00 0.00	0.84 0.46	0.09 0.10	0.25 0.14	0.03 0.03
Cumulative flow per cycle, kg	5.5 8.4	670.0 1018.4	0.9 1.1	421.2 231.7	46.1 51.3	127.4 69.3	13.0 16.4

Following the discussion in Section 3.1, the major difference between the adiabatic and isothermal cases is the higher space velocity, and higher feed flow rates, in the isothermal case. As a result of the higher CO_2 and H_2 flow rates during the reaction step, methanol is produced at a higher rate in the isothermal configuration. As found in Table 10, the average methanol production rate is 1.3 and 2.0 kg/s in the adiabatic and isothermal cases, respectively. Methanol is also produced at higher selectivity due to the lower reactor temperature in the water-cooled isothermal reactor, which limits the production of CO via the RWGS. This can be seen from the lower CO flow rate in the purge gas in the isothermal case. It is noted that experimental studies have shown the importance of limiting the reactor temperature during sorption-enhanced methanol synthesis to limit CO formation [32]. Methanol selectivity was also found to increase with increasing pressure. Thus, further optimization efforts should also investigate the reactor pressure.

During regeneration, the component outlet flow rates are again higher in the isothermal case due to the higher purge gas flow rate. The difference in the depressurization outlet flow rates is due to the manual adjustment performed in order to close the overall mass balances (Section 2.2.3). In the adiabatic case, the depressurization flow rates were reduced by 33%, while in the isothermal case, an increase of 46% was required. The exact source of deviation in the corresponding mass balances prior to this adjustment are unknown, and the final depressurization flow rates should be viewed cautiously due to these corrections.

Fig. 6 illustrates the cyclic nature of the process by presenting the variation in component inlet and outlet molar flow rates over time during the reaction and displacement steps. Due to more favorable results in terms of the production cost estimate (Section 3.4), the plots are only shown for the adiabatic case. However, similar results were found for the isothermal case. The displacement steps are identified by the large peaks in CO_2 input. Methanol is produced continuously with minor variation in the production rate as one of the three reactors remains at the reaction or displacement step at all times in the suggested cycle design (Section 2.2.1). The methanol flow rate peaks at the beginning of the reaction step when the production rate is maximized by maximum

Table 9
Component maximum, average and cumulative flow rates at process outlet streams over the regeneration and depressurization steps, in the adiabatic (figures above) and isothermal (figures below) reactor configuration. Components with minor flows (cumulative <1 kg) are not included.

Step	Regeneration			Depressurization			
Outlet stream	Gas outlet			Condensate	Outlet gas		
Component	CO_2	H_2	CO	Water	CO_2	CO	Water
Maximum flow rate, kg/s	0.81	0.00	0.00	2.49	5.55	0.07	0.03
	1.24	0.00	0.00	3.12	10.94	0.11	0.03
Average flow rate, kg/s	0.81	0.00	0.00	0.50	2.77	0.03	0.02
	1.24	0.00	0.00	1.01	5.47	0.06	0.02
Cumulative flow per cycle, kg	407.3	0.2	0.3	251.7	1387.2	17.1	8.3
	620.3	0.3	0.2	503.7	2733.9	27.8	8.3

Table 10
Mass balance and process performance summary in the adiabatic and isothermal configuration, and comparison to a reference process representing conventional CO_2 hydrogenation [40]. Flow rates for sorption-enhanced processes are average values over the cycle.

Mass flow, kg/h	Adiabatic	Isothermal	Reference process
Input flows			
CO_2 input	6373	10138	
CO_2 make-up	2384	3683	3882
(kg/kg MeOH)	(1.8)	(1.8)	(1.7)
H_2 input	354	512.4	
H_2 make-up	268	406	533
(kg/kg MeOH)	(0.2)	(0.2)	(0.2)
Recycle flows			
CO_2 recycled	3988	6455	
H_2 recycled	87	107	
Output flows			
Methanol output	1340	2037	2272
CO_2 purged	443	717	560
CO_2 from waste heat combustion	938	1140	177
Total CO_2 output	1381	1857	743
(kg/kg MeOH)	(1.0)	(0.9)	(0.3)
Methanol purity, w-%	99.1%	99.1%	99.7%
Methanol yield (carbon basis)	77.2%	76.0%	80.9%
Methanol yield (hydrogen basis)	94.5%	94.8%	90.6%

water adsorption by the regenerated adsorbent, and during the displacement when remaining methanol is removed from the catalyst/adsorbent bed by the CO_2 purge. Due to the near-complete water adsorption, the amount of water contained in the condensed product stream is negligible (Table 11). Losses of methanol with the purge gas are also negligible.

Water production remains low due to the presented operating scheme based on avoidance of water breakthrough, and production of high-purity crude methanol directly from the reactor loop. Same analysis carried out at lower methanol purity target would obviously increase the water output rate, but also result in higher average methanol production rate over the cycle, as the duration of the reaction step could be increased. As found in Fig. 6, the purge gas flow rates peak during the displacement step when gases are removed by the CO_2 purge. Fig. 7 presents the variation in input and output flow rates during the regeneration step. Again, the results are shown for the adiabatic case but are essentially identical for the isothermal case. Here, the input and output of CO_2 as purge gas remains essentially constant as one of the three reactors is kept continuously in the regeneration mode. The output of water removed from the regeneration loop peaks during the beginning of the regeneration step when the amount of water desorbed and released from the reactor bed is at the maximum. Losses of H_2 and CO in the purge gas during regeneration are negligible.

A summary of the process mass balances for the adiabatic and isothermal cases is given in Table 12. For comparison, comparable results from the reference CO_2 hydrogenation process are included. The methanol yield, on both carbon or hydrogen basis, are very similar in the sorption-enhanced cases resulting in identical specific CO_2 and H_2 make-up rates per rate of methanol produced. The recycle and make-up rates are calculated at the assumed 90% recovery of both CO_2 and H_2 at the gas separation step. The higher gas input rates (space velocity) in the isothermal case (Section 3.1) results in a higher methanol production rate compared to the adiabatic case.

4.3. Process energy balances

Table 11 summarizes the heat inputs and outputs, and utility demands in the adiabatic and isothermal cases. Here, pre-heat refers to the amount of additional heat required for pre-heating the reactor inlet gas (or purge gas during regeneration) following heat integration with reactor outlet. During the reaction and displacement steps, methanol and water are condensed using cooling water, while during regeneration chilled water (or other low-temperature coolant) is required to condense the water removed from the reactors. The larger heating and cooling duties in the isothermal case are explained by higher flow rates.

Electricity is consumed by compression of the H_2 input during the reaction and repressurization steps, and the recycle compressors required during reaction and regeneration. Table 12 presents the resulting electricity demands. The total electricity demand is clearly dominated by the regeneration recycle compressor. This is due to the significant rate of purge gas (CO_2) circulated during the regeneration step.

As presented in Table 13, both process configurations result in a net output of heat following heat utilization within the processes. Heat is generated by combustion of purge gases and also by reactor steam generation in the isothermal case. Due to the latter, the isothermal configuration results in a more significant heat output.

Fig. 8 illustrates the cyclic nature of the process energy balance. In the adiabatic case, the pre-heat steam demand during the reaction and regeneration step varies following change in the reactor bed and outlet flow temperature. In the isothermal case, the variation in heat demand is less significant due to the nearly constant reactor temperature. The pre-heat demand during reaction is higher in the isothermal case as less heat is available by direct heat transfer from the reactor outlet due to the lower outlet temperature. However, this is offset by the additional heat extracted by steam generation in the isothermal reactors. In both cases, additional heat is available from waste heat combustion. Available waste heat peaks during the displacement step when combustible gases are removed at high rate.

A summary of the process energy balance is given in Table 14. The specific utility demands per amount of methanol produced are very similar in the adiabatic and isothermal cases. The amount of surplus steam extracted from the process is much more significant in the isothermal case due to conversion of reaction heat into steam in the water-cooled reactor configuration.

4.4. Production costs

Fig. 9 presents a comparison of the total methanol production cost

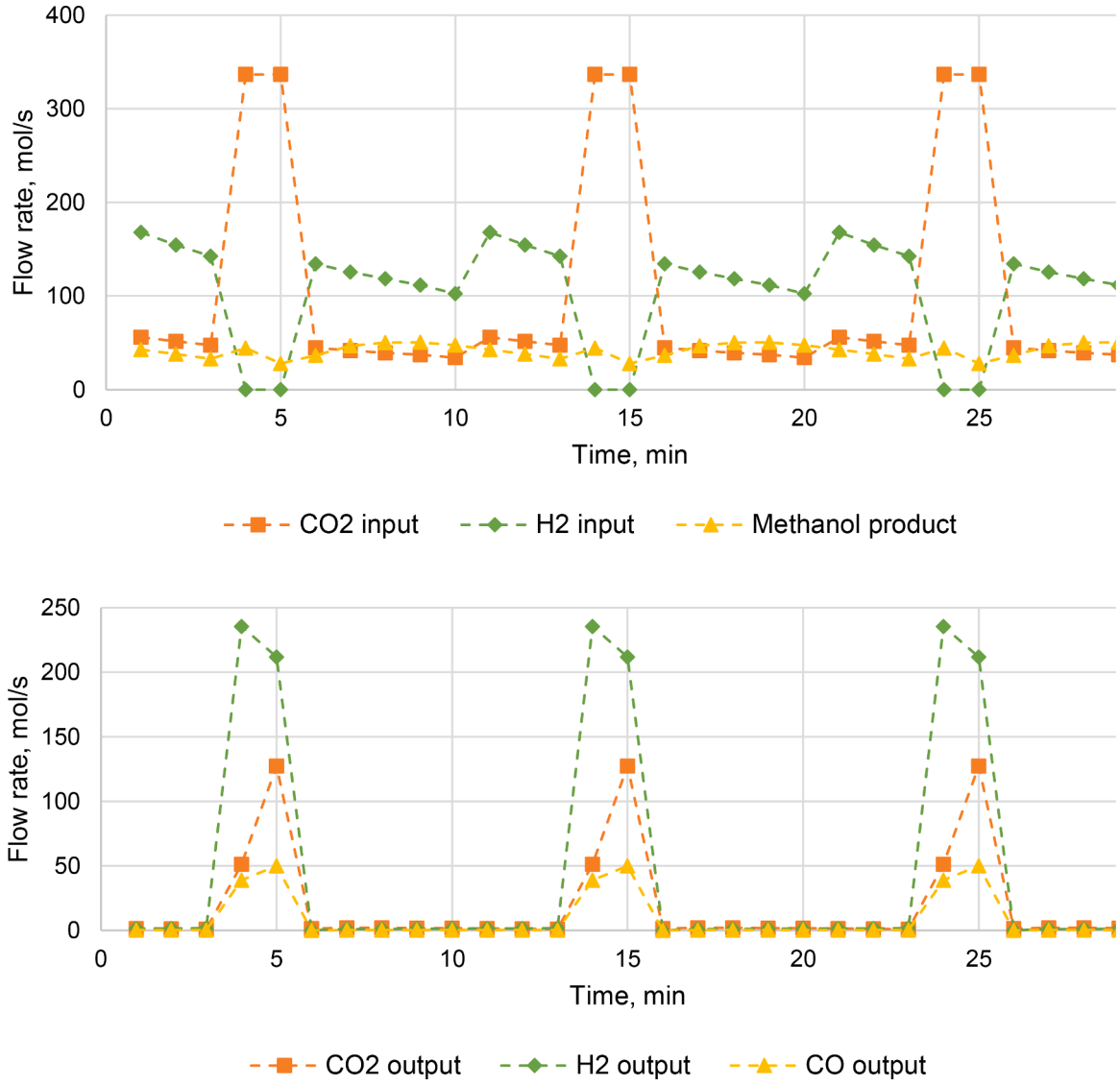

Fig. 6. Component molar flow rates over cycle time during the reaction and displacement steps, in the adiabatic reactor configuration. Above: reactant inputs and condensed methanol product; below: purge gas following product condensation. CO_2 and H_2 inputs refer to combined input of fresh (make-up) and recycled gases to the reactor loop. Flow rates are calculated at time resolution of 1 min, with lines added for visualization. Components with negligible flow rates are not included.

Table 11
Heat inputs and outputs over the cycle in the adiabatic (figures above) and isothermal (figures below) configuration.

Process step	Reaction + displacement		Regeneration	
Energy input/ output(utility)	Pre-heat (MP steam)	Condenser (cooling water)	Pre-heat (MP steam)	Condenser (chilled water)
Maximum duty, kW	892 684	602 928	800 1084	4063 5582
Average duty, kW	172 375	493 680	593 1082	2430 3827
Cumulative energy per cycle, kWh	86 188	246 340	296 541	1215 1914

via the suggested sorption-enhanced process in the adiabatic and isothermal reactor configurations. Equipment specifications and installed capital costs for the sorption-enhanced processes are presented in Tables SIV–SV (Supplementary information). In addition, the costs are compared to a reference process representing the conventional gas-phase fixed-bed technology for the hydrogenation of CO_2 to methanol. The costs for the reference process were estimated in a previous publication [40] based on similar costing methodology and main assumptions using the same costs for hydrogen and CO_2 as in the present study. The reference process was scaled down from the original capacity of 18 kt/a methanol to the scale of the adiabatic sorption-enhanced process with the CAPEX costs scaling factor of 0.67.

Of the sorption-enhanced processes, the adiabatic option is found more competitive, at the cost level of 1085 €/t compared to 1255 €/t for the isothermal case. While the variable costs are essentially identical in the both cases, the overall cost in the isothermal configuration is higher due to higher capital costs. The difference in the specific capital cost (per t of methanol produced) is explained by the higher cost of the isothermal reactors, constituting tubular heat exchanger reactors, compared to the simpler adiabatic packed-bed reactors. This is illustrated by the contributions to total CAPEX allocated by type of equipment, as shown in Fig. 10. It is also noted that the capital cost distribution in the adiabatic case is very similar to the reference process.

The production cost for the adiabatic configuration is nearly equal to the reference process (1089 €/t). The cost estimate for the reference

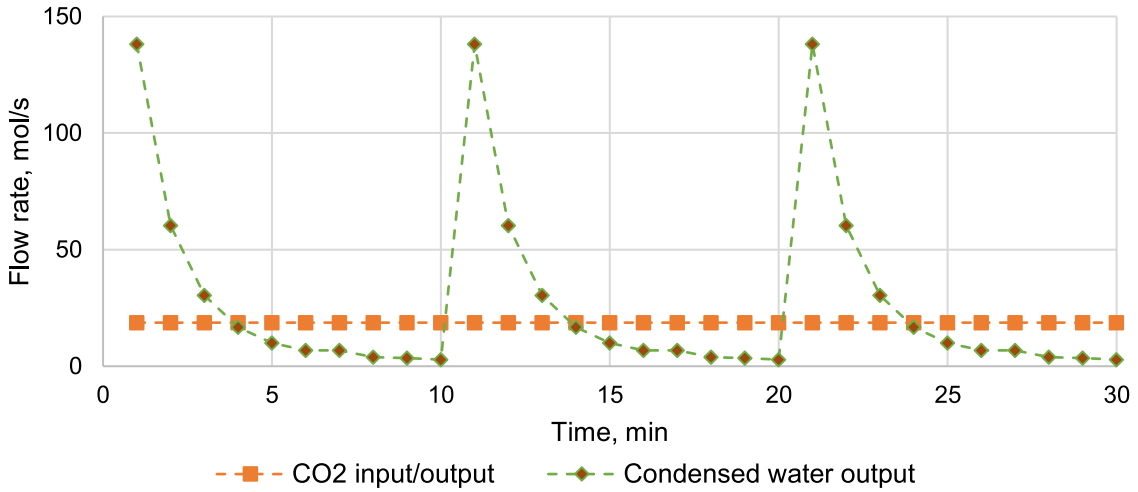

Fig. 7. Component molar flow rates over cycle time during the regeneration step in the adiabatic reactor configuration. Flow rates are calculated at time resolution of 1 min, with lines added for visualization. Components with negligible flow rates are not included.

Table 12
Electricity demand over the cycle for the adiabatic (figures above) and isothermal (figures below) configuration.

Process step	Reaction + displacement		Regeneration	Repressurization
Equipment	H_2 compressor	Recycle compressor	Recycle compressor	H_2 compressor
Maximum duty, kW	77 117	7 11	1463 2189	64 64
Average duty, kW	49 84	5 8	1440 2185	32 32
Cumulative energy per cycle, kWh	24 42	2 4	720 1092	16 16

Table 13
Heat generation over the cycle in the adiabatic (figures above) and isothermal (figures below) reactor configuration. Surplus heat refers to the amount of excess heat from reactor cooling and waste heat combustion remaining after utilization of heat within the process.

Energy input/output	Waste heat (steam) generated	Reactor steam output	Surplus heat
Maximum duty, MW	4.9 3.5	- 9.1	4.5 9.5
Average duty, MW	1.2 1.6	- 7.0	0.4 7.1
Cumulative energy per cycle, MWh	0.6 0.8	- 1.5	0.2 3.6

process is comparable to other estimates for CO_2-based methanol synthesis under present technological and economic conditions [41–44]. The major difference between these processes is the higher capital costs of the sorption-enhanced process. Compared to the reference process, the capital costs of the sorption-enhanced process in the present configuration are reduced by the elimination of distillation columns. However, reactor costs are higher both due to the parallel reactors required, and the larger reactor volume due to inclusion of catalyst and adsorbent within the same fixed bed. The capital costs are also increased by the cyclic operation and significant variation in flow rates over cycle time (Figs. 6 and 7), as all equipment needs to be sized for the maximum flow rates. Capital costs are especially increased by the large purge gas flow rate during regeneration, resulting in high cost for the recycle compressors.

However, the difference in capital costs is compensated by the lower operating costs of sorption-enhanced process. More specifically, the specific hydrogen costs are reduced by more efficient utilization of hydrogen input. This is evident from the methanol yield calculated on hydrogen-basis, which is 95% in the sorption-enhanced process configurations, and 91% in the reference process. This difference is due to the higher single-pass conversion in the sorption-enhanced process enabled by water sorption, which is a major benefit of the sorption-enhanced process. Similar to any CO_2 hydrogenation processes, the production cost of the sorption-enhanced process is significantly sensitive to the hydrogen cost, as found from the sensitivity analysis presented in Fig. 11.

It could thus be concluded that sorption-enhanced methanol synthesis does not seem to provide economic benefits, as opposed to the case of sorption-enhanced DME synthesis studied by Skorikova et al. [24]. In their case, the DME production cost via the sorption-enhanced process was estimated significantly lower (1300 €/t) compared to average reported cost of CO_2-based DME production (2700 €/t).

However, it must be emphasized that the present process represents the first design for the sorption enhanced methanol process giving promising results with costs approaching the reference process. We expect that there is a lot of space for further process development and optimization. The suggested process represents a single optimization case using the methanol production rate, and not the overall production cost as the optimization target. Furthermore, the process is optimized under the boundary condition of yielding >99 w-% crude methanol without distillation. This demonstrates the flexibility of this process but may not constitute the economically optimal operating principle. Decreasing the purity target would increase the production rate and result in a lower specific cost, but only if the lower purity is sufficient without further purification. This would be highly dependent on the intended methanol application. We have previously carried out optimization of the methanol production rate versus the purity target [23]. Ideally, such optimization should also be carried out with the overall production cost as the objective function.

Future work should also consider catalyst and adsorbent deactivation. Any deactivation phenomena has not been observed during our experimental work [32]. Specific deactivation studies on sorption-enhanced methanol synthesis have not been carried out in our knowledge. As deactivation processes are often relatively slow, dedicated experiments at long run times would likely be required to observe such effects. Both potentially favorable and unfavorable deactivation characteristics for sorption-enhanced methanol synthesis, compared to conventional CO_2-based methanol synthesis, can be identified. The presence of zeolite catalysts could lead to harmful side reactions (e.g.,

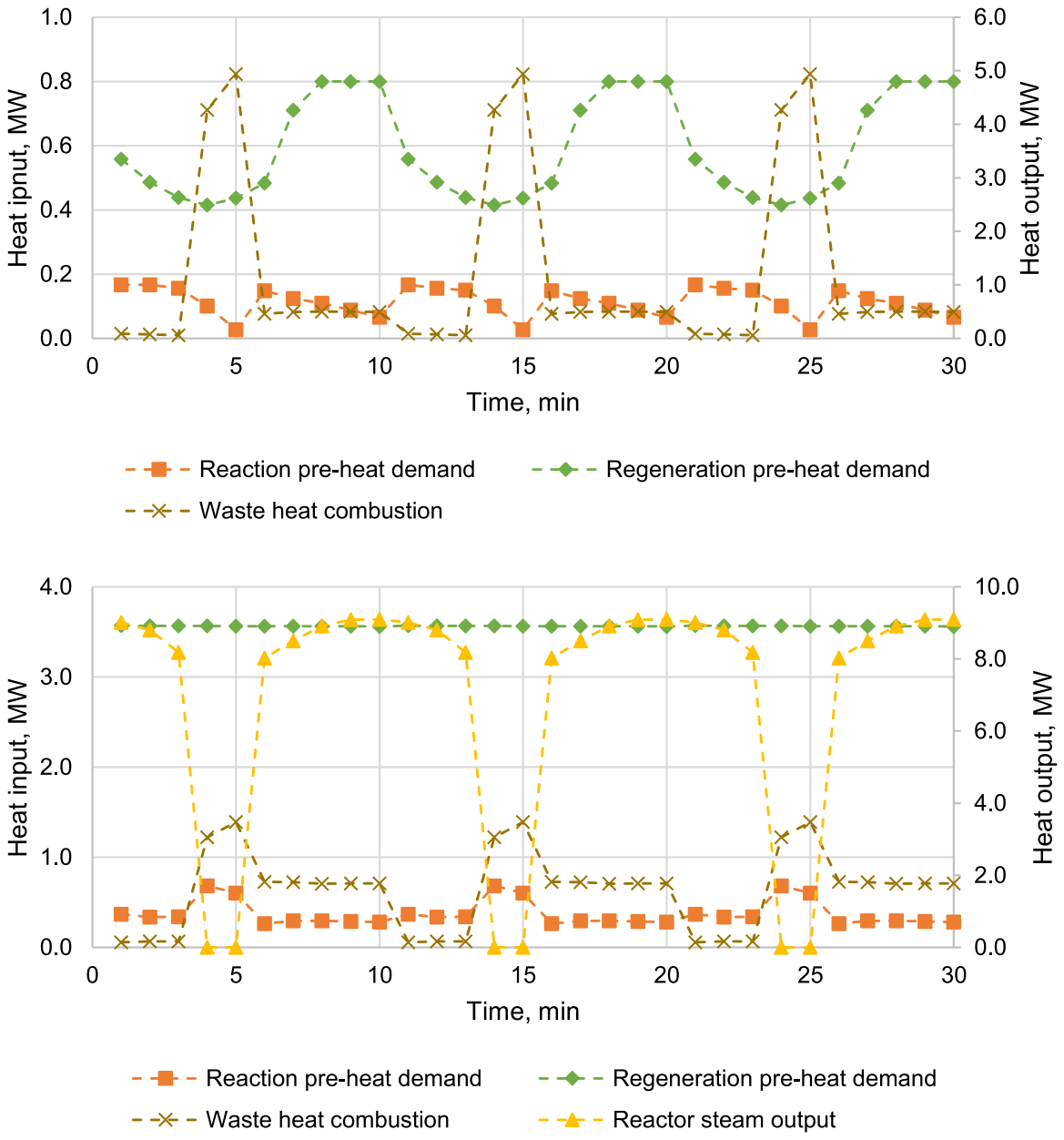

Fig. 8. Heat inputs and outputs over cycle time for the adiabatic (above) and isothermal (below) reactor configurations. Heat outputs on secondary axis. Waste heat and reactor steam output are calculated assuming 85% efficiency. Heat duties are calculated at time resolution of 1 min, with lines added for visualization

Table 14
Energy balance summary in the adiabatic and isothermal configuration, and comparison to a reference process representing conventional CO_2 hydrogenation [40]. Results for sorption-enhanced processes are average values over the cycle.

Duty, MW (Energy, kWh/kg MeOH)	Adiabatic	Isothermal	Reference process
Steam generation	1.2	8.6	(1.3)
Steam consumption	0.8	3.9	-
Steam surplus	0.4 (0.3)	4.6 (2.3)	(1.3)
Cooling water requirement	0.5 (0.4)	0.7 (0.3)	(0.9)
Chilled water requirement	2.4 (1.8)	3.8 (1.9)	-
Electricity consumption	1.5 (1.1)	2.3 (1.1)	(0.2)

coking) via further methanol conversion. However, this should be limited by the small pore size of the adsorbent, as only the particle outer surface would be available for reactions involving methanol (or any larger molecules). On the other hand, the adsorption of water could be beneficial as water is known to accelerate sintering of methanol synthesis catalysts [45].

The present study is based on the relatively rigorous modelling and optimization of the reactor loop but the downstream separation section is not designed and modelled at similar rigor. The present separation and adsorbent regeneration schemes could thus be significantly improved. Economic operation of the process requires the effective utilization of CO_2 and H_2 and minimizing unnecessary losses. The large CO_2 and H_2 flows during the displacement and regeneration steps in the present configurations would lead to excessive reactant losses and poor methanol yield without the gas separation and recycle scheme discussed in Section 2.2.4. Here, we did not provide a detailed design for the gas separation section as it is feasible that the gases could be directly

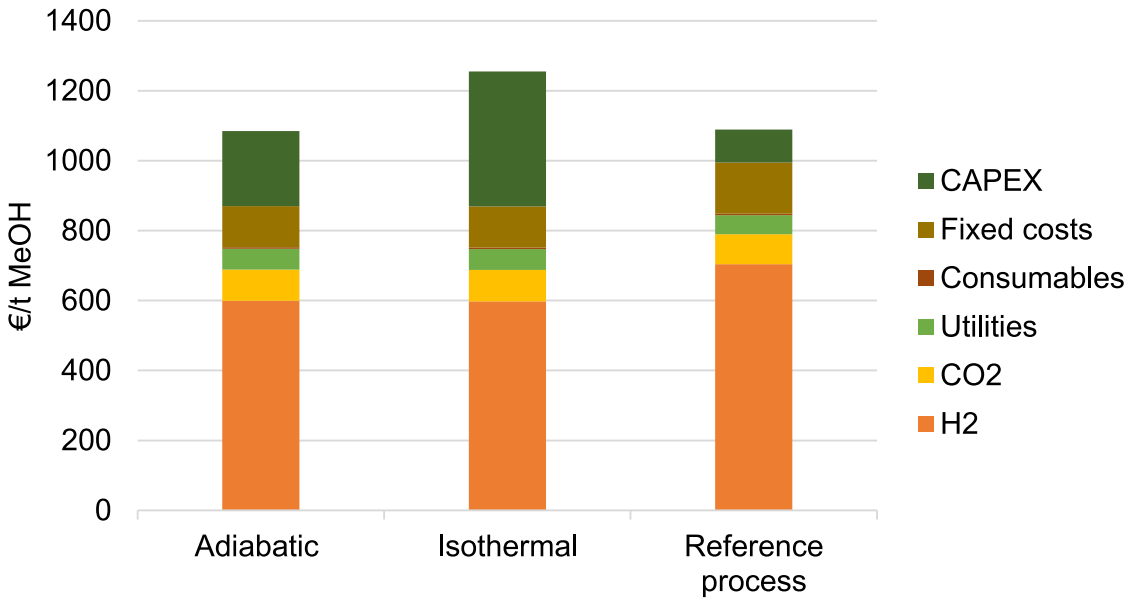

Fig. 9. Methanol production cost via the sorption-enhanced methanol synthesis process in the adiabatic and isothermal reactor configurations, and comparison to a reference process [40] representing conventional CO_2 hydrogenation to methanol.

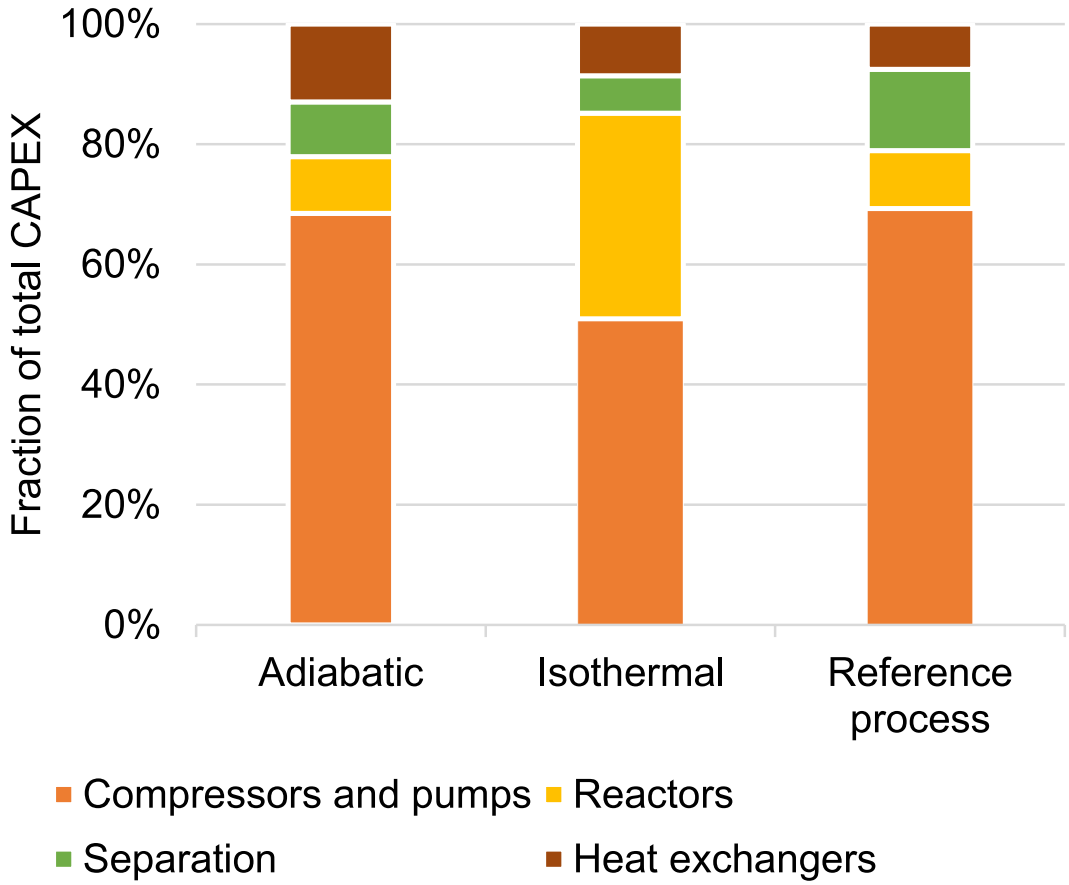

Fig. 10. Fraction of total capital costs allocated by equipment type for the sorption-enhanced methanol synthesis process in the adiabatic and isothermal reactor configurations, and comparison to a reference process [40] representing conventional CO_2 hydrogenation to methanol.

recycled with no or minimum separation or purification required. A sensitivity analysis was performed to measure the impact of gas recovery and losses on the methanol production cost (Fig. 12). For instance, decreasing the CO_2 or H_2 recovery from 90% to 50% would increase the total production cost by 6% or 8%, respectively, in the adiabatic case.

It should be noted that the present analysis does not consider any costs for the hypothetical gas separation scheme. We also investigated the effect of the hypothetical gas separation costs on the overall methanol production cost. For instance, at the default CO_2 and H_2 input costs and recovery fractions of 90%, setting the separation costs at 50% of the

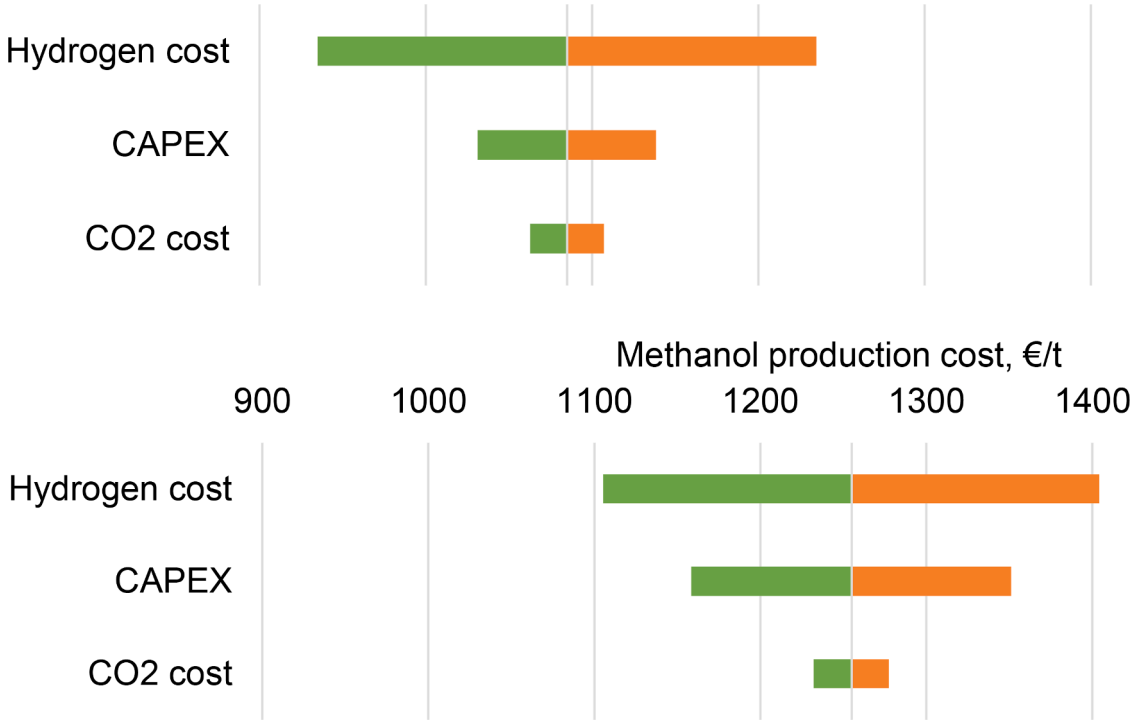

Fig. 11. Methanol production cost sensitivity analysis in the adiabatic (above) and isothermal configuration (below). Each parameter changed by +/-25% from the base value. Base values: hydrogen cost 3000 €/t, CO_2 cost 50 €/t, total capital cost (CAPEX) 22.6 M€ (adiabatic) or 40.6 M€ (isothermal).

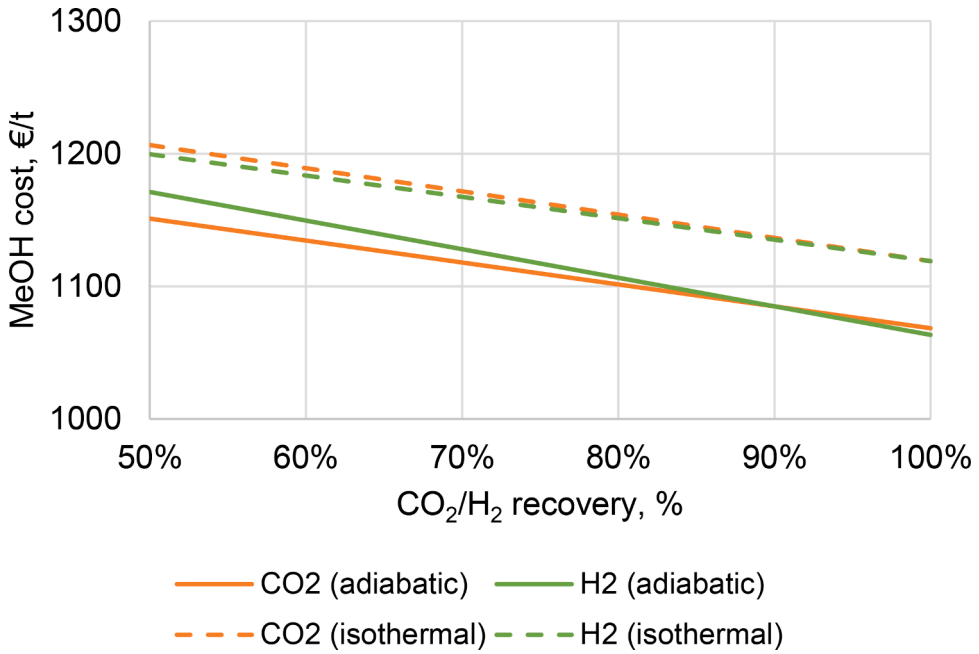

Fig. 12. Sensitivity of methanol production cost to the recovery of CO_2 and H_2 via the gas recycle scheme. Base value for recovery is 90% for both CO_2 and H_2.

input cost (i.e., 25 €/t for CO_2 and 1500 €/t for H_2), would increase the methanol production cost to 1256 €/t or 1413 €/t in the adiabatic and isothermal case, respectively.

5. Conclusion and suggestions

In this study, a sorption-enhanced process for hydrogenation of CO_2 to methanol was designed and investigated. The modelling methodology combined dynamic modelling and optimization of the reactor loop within the cyclic process, combined with pseudo-steady state modelling of the overall process. The latter was performed at time resolution of one minute, using outputs from the dynamic model at each time point as inputs to the steady-state model. By this approach, the dynamic mass and energy balances of the process could be approximated with satisfactory resolution and accuracy. In addition, the preliminary feasibility of the developed process was estimated by means of a techno-economic analysis.

The continuous adsorption of water in the sorption-enhanced process

allows adjustment of the water content in the crude methanol product and the production of highly pure methanol without downstream distillation. Here, this capability was demonstrated by setting the crude methanol purity at >99%. Under this boundary condition, the reactor cycle was designed to maximize the methanol production rate. The cycle and process were modelled in two reactor configurations, based on the use of either adiabatic or isothermal, water-cooled reactors.

The adiabatic configuration was found more competitive in terms of the overall methanol production cost due to higher capital costs for the isothermal case. The overall production cost for the adiabatic case was found comparable to a reference process representing conventional CO_2 hydrogenation to methanol. Compared to the reference process, the specific capital costs are higher, but this difference is offset by more efficient utilization of hydrogen resulting in reduced operating costs for the sorption-enhanced process. While the suggested process does not require distillation columns, the capital costs are increased by the need of multiple reactors and higher reactor volume due to inclusion of the adsorbent. The costs are also increased due to significant variation in component flow rates over the cycle, as all equipment needs to be sized based on the maximum (and not average) flow rates.

The production costs of the sorption-enhanced process could be reduced by further optimization in terms of the cycle design and timing, reactor configuration, and overall process design including product separation. Optimization in terms of the production cost should be carried out over the complete process, in contrast to the present case where only the reactor configuration was optimized to maximize the production rate. The production cost might be minimized at significantly different cycle design and operating conditions from those suggested in this study.

The operating principle suggested here, based on the production of purified methanol without distillation, is an interesting option but may not constitute the economically optimal case. As the present process allows adjusting the water content in the crude methanol product, the separation and purification scheme could be designed and optimized depending on the crude methanol purity. The methanol production rate could be maximized by producing methanol at high water content and adding a distillation train. On the other hand, decreased water content in crude methanol might make alternative separation options more favorable. Various options, for example membrane separation or adsorptive drying should be investigated, and the optimum selection of separation processes as a function of the crude methanol composition should be identified.

One of the key issues to achieve lower costs and profitable methanol production is to have high production rate per fixed-bed volume. In the current design with a physical mixture of catalyst and adsorbent, the volumetric production rate is inherently low. This could be mitigated by developing novel catalysts where the reaction and adsorption functions are combined. Such catalysts have been already developed and tested for simultaneous production of methanol and dimethyl ether [46]. Another point is that the sorption-enhanced process is limited by the adsorption capacity of the zeolite adsorbent at high reaction temperatures. Development of novel water-selective adsorptive materials for high-temperature operation that could decrease the production costs significantly [47,48]. In addition, the materials should be simple to regenerate, preferably by pressure-swing cycles to minimize the energy and time required for regeneration and to maximize the methanol productivity over the cycle. Thus, the specific methanol production rate over the cycle could be increased, and the specific operating costs decreased [47,48].

Declaration of Competing Interest

The authors declare that they have no known competing financial interests or personal relationships that could have appeared to influence the work reported in this paper.

Data for reference

Data will be made available on request.

Acknowledgments

The work was mostly performed under the P2XEnable collaboration project primarily funded by Business Finland.

Supplementary materials

Supplementary material associated with this article can be found, in the online version, at doi:10.1016/j.cep.2022.109052.

References

[1] M. Aresta, A. Dibenedetto, A. Angelini, Catalysis for the valorization of exhaust carbon: from CO_2 to chemicals, materials, and fuels. technological use of CO2, Chem. Rev. 114 (2014) 1709–1742, https://doi.org/10.1021/cr4002758.
[2] C. Graves, S.D. Ebbesen, M. Mogensen, K.S. Lackner, Sustainable hydrocarbon fuels by recycling CO_2 and H2O with renewable or nuclear energy, Renew. Sustain. Energy Rev. 15 (2011) 1–23, https://doi.org/10.1016/j.rser.2010.07.014.
[3] F. Schüth, Chemical compounds for energy storage, Chem. Ing. Tech. 83 (2011) 1984–1993, https://doi.org/10.1002/cite.201100147.
[4] A. Kätelhön, R. Meys, S. Deutz, S. Suh, A. Bardow, Climate change mitigation potential of carbon capture and utilization in the chemical industry, Proc. Natl. Acad. Sci. U. S. A. 166 (2019) 11187–11194, https://doi.org/10.1073/pnas.1821029116.
[5] C. Ampelli, S. Perathoner, G. Centi, CO2 utilization: an enabling element to move to a resource-and energy-efficient chemical and fuel production, Philos. Trans. R. Soc. A 373 (2015), https://doi.org/10.1098/rsta.2014.0177.
[6] A. Goeppert, M. Czaun, J.P. Jones, G.K. Surya Prakash, G.A. Olah, Recycling of carbon dioxide to methanol and derived products-closing the loop, Chem. Soc. Rev. 43 (2014) 7995–8048, https://doi.org/10.1039/c4cs00122b.
[7] M. Bertau, H.J. Wernicke, F. Schmidt, Methanol Utilisation Technologies, in: Methanol: the Basic Chemical and Energy Feedstock of the Future: Asinger's Vision Today, Springer, Berlin Heidelberg, 2014, pp. 327–601, https://doi.org/10.1007/978-3-642-39709-7_6.
[8] D. Sheldon, Methanol production - a technical history, Johns. Matthey Technol. Rev. 61 (2017) 172–182, https://doi.org/10.1595/205651317X695622.
[9] V. Dieterich, A. Buttler, A. Hanel, H. Spliethoff, S. Fendt, Power-to-liquid via synthesis of methanol, DME or Fischer–Tropsch-fuels: a review, Energy Environ. Sci. 13 (2020) 3207–3252, https://doi.org/10.1039/d0ee01187h.
[10] J. Ott, V. Gronemann, F. Pontzen, E. Fiedler, G. Grossmann, D.B. Kersebohm, G. Weiss, C. Witte, in Methanol, Ullmann's Encyclopedia of Industrial Chemistry, Wiley-VCH Verlag GmbH & Co. KGaA, Weinheim, Germany, 2012, https://doi.org/10.1002/14356007.a16_465.pub3.
[11] O. Martin, J. Pérez-Ramírez, New and revisited insights into the promotion of methanol synthesis catalysts by CO_2, Catal. Sci. Technol. 3 (2013) 3343–3352, https://doi.org/10.1039/c3cy00573a.
[12] A. Bansode, A. Urakawa, Towards full one-pass conversion of carbon dioxide to methanol and methanol-derived products, J. Catal. 309 (2014) 66–70, https://doi.org/10.1016/j.jcat.2013.09.005.
[13] J.G. van Bennekom, R.H. Venderbosch, J.G.M. Winkelman, E. Wilbers, D. Assink, K.P.J. Lemmens, H.J. Heeres, Methanol synthesis beyond chemical equilibrium, Chem. Eng. Sci. 87 (2013) 204–208, https://doi.org/10.1016/j.ces.2012.10.013.
[14] M.J. Bos, D.W.F. Brilman, A novel condensation reactor for efficient CO_2 to methanol conversion for storage of renewable electric energy, Chem. Eng. J. 278 (2015) 527–532, https://doi.org/10.1016/j.cej.2014.10.059.
[15] N. Tsubaki, M. Ito, K. Fujimoto, A new method of low-temperature methanol synthesis, J. Catal. 197 (2001) 224–227, https://doi.org/10.1006/JCAT.2000.3077.
[16] Z. Li, Y. Deng, N. Dewangan, J. Hu, Z. Wang, X. Tan, S. Liu, S. Kawi, High temperature water permeable membrane reactors for CO_2 utilization, Chem. Eng. J. 420 (2021), 129834,, https://doi.org/10.1016/j.cej.2021.129834.
[17] J. van Kampen, J. Boon, M. van Sint Annaland, Separation enhanced methanol and dimethyl ether synthesis, J. Mater. Chem. A 9 (2021) 14627–14629, https://doi.org/10.1039/D1TA03405G.
[18] J. Boon, K. Coenen, E. van Dijk, P. Cobden, F. Gallucci, M. van Sint Annaland, Sorption-enhanced water–gas shift, in: 2017: pp. 1–96. 10.1016/bs.ache.2017.07.004.
[19] A. Borgschulte, N. Gallandat, B. Probst, R. Suter, E. Callini, D. Ferri, Y. Arroyo, R. Erni, H. Geerlings, A. Züttel, Sorption enhanced CO_2 methanation, Phys. Chem. Chem. Phys. 15 (2013) 9620, https://doi.org/10.1039/c3cp51408k.
[20] A. Zachopoulos, E. Heracleous, Overcoming the equilibrium barriers of CO2 hydrogenation to methanol via water sorption: a thermodynamic analysis, J. CO2 Util. 21 (2017) 360–367, https://doi.org/10.1016/j.jcou.2017.06.007.
[21] M. Bayat, Z. Dehghani, M.R. Rahimpour, Sorption-enhanced methanol synthesis in a dual-bed reactor: dynamic modeling and simulation, J. Taiwan Inst. Chem. Eng. 45 (2014) 2307–2318, https://doi.org/10.1016/j.jtice.2014.04.023.

[22] A. Arora, S.S. Iyer, I. Bajaj, M.M.F. Hasan, Optimal methanol production via sorption-enhanced reaction process, Ind. Eng. Chem. Res. 57 (2018) 14143–14161, https://doi.org/10.1021/acs.iecr.8b02543.
[23] P. Maksimov, H. Nieminen, A. Laari, T. Koiranen, Sorption enhanced carbon dioxide hydrogenation to methanol: process design and optimization, Chem. Eng. Sci. (2022), 117498,, https://doi.org/10.1016/j.ces.2022.117498.
[24] G. Skorikova, M. Saric, S.N. Sluijter, J. van Kampen, C. Sánchez-Martínez, J. Boon, The techno-economic benefit of sorption enhancement: evaluation of sorption-enhanced dimethyl ether synthesis for CO2 utilization, Front. Chem. Eng. 2 (2020) 1–11, https://doi.org/10.3389/fceng.2020.594884.
[25] X. Zhen, Methanol as an internal combustion on engine fuel. Methanol: Science and Engineering, Elsevier, 2018, pp. 313–337, https://doi.org/10.1016/B978-0-444-63903-5.00011-X.
[26] F. Samimi, M.R. Rahimpour, Direct methanol fuel cell. Methanol: Science and Engineering, Elsevier, 2018, pp. 381–397, https://doi.org/10.1016/B978-0-444-63903-5.00014-5.
[27] P. Maksimov, H. Nieminen, A. Laari, T. Koiranen, Sorption enhanced carbon dioxide hydrogenation to methanol: process design and optimization [Submitted for Review], (2021).
[28] P. Maksimov, A. Laari, V. Ruuskanen, T. Koiranen, J. Ahola, Methanol synthesis through sorption enhanced carbon dioxide hydrogenation, Chem. Eng. J. 418 (2021), https://doi.org/10.1016/j.cej.2021.129290.
[29] H. Graaf, E.J. Stamhuis, A.A.C.M. Beenackers, Kinetics of low-pressure methanol synthesis, Chem. Eng. Sci. 43 (1988) 3185–3195.
[30] G.H. Graaf, J.G.M. Winkelman, Chemical equilibria in methanol synthesis including the water-gas shift reaction: a critical reassessment, Ind. Eng. Chem. Res. (2016), https://doi.org/10.1021/acs.iecr.6b00815.
[31] P. Maksimov, A. Laari, V. Ruuskanen, T. Koiranen, J. Ahola, Gas phase methanol synthesis with Raman spectroscopy for gas composition monitoring, RSC Adv. 10 (2020) 23690–23701, https://doi.org/10.1039/d0ra04455e.
[32] P. Maksimov, A. Laari, V. Ruuskanen, T. Koiranen, J. Ahola, Methanol synthesis through sorption enhanced carbon dioxide hydrogenation, Chem. Eng. J. 418 (2021), https://doi.org/10.1016/j.cej.2021.129290.
[33] B.A. Finlayson, Introduction to Chemical Engineering Computing, Wiley-Interscience, 2006.
[34] R.R. Akberov, Calculating the vapor-liquid phase equilibrium for multicomponent systems using the Soave-Redlich-Kwong equation, Theor. Found. Chem. Eng. 45 (2011) 312–318, https://doi.org/10.1134/S004057951103002X.
[35] G. Soave, Equilibrium Constants From a Modified Redkh-Kwong Equation of State, Pergamon Press, 1972.
[36] J. Skrzypek, M. Lachowska, D. Serafin, Methanol synthesis from CO_2 and H_2: dependence of equilibrium conversions and exit equilibrium concentrations of components on the main process variables, Chem. Eng. Sci. 45 (1990) 89–96, https://doi.org/10.1016/0009-2509(90)87083-5.
[37] É.S. Van-Dal, C. Bouallou, Design and simulation of a methanol production plant from CO2 hydrogenation, J. Clean. Prod. 57 (2013) 38–45, https://doi.org/10.1016/j.jclepro.2013.06.008.
[38] I. Hannula, Co-production of synthetic fuels and district heat from biomass residues, carbon dioxide and electricity: performance and cost analysis, Biomass Bioenergy 74 (2015) 26–46, https://doi.org/10.1016/j.biombioe.2015.01.006.
[39] W. Boll, G. Hochgesand, C. Higman, E. Supp, P. Kalteier, W.-D. Müller, M. Kriebel, H. Schlichting, H. Tanz, Gas production, 3. Gas treating, Ullmann's Encycl. Ind. Chem. (2011), https://doi.org/10.1002/14356007.o12_o02.
[40] H. Nieminen, A. Laari, T. Koiranen, CO2 hydrogenation to methanol by a liquid-phase process with alcoholic solvents: a techno-economic analysis, Processes 7 (2019) 405, https://doi.org/10.3390/pr7070405.
[41] M. Pérez-Fortes, J.C. Schöneberger, A. Boulamanti, E. Tzimas, Methanol synthesis using captured CO_2 as raw material: techno-economic and environmental assessment, Appl. Energy 161 (2016) 718–732, https://doi.org/10.1016/j.apenergy.2015.07.067.
[42] C. Hank, S. Gelpke, A. Schnabl, R.J. White, J. Full, N. Wiebe, T. Smolinka, A. Schaadt, H.M. Henning, C. Hebling, Economics & carbon dioxide avoidance cost of methanol production based on renewable hydrogen and recycled carbon dioxide-power-to-methanol, Sustain. Energy Fuels 2 (2018) 1244–1261, https://doi.org/10.1039/c8se00032h.
[43] M.A. Adnan, M.G. Kibria, Comparative techno-economic and life-cycle assessment of power-to-methanol synthesis pathways, Appl. Energy 278 (2020), https://doi.org/10.1016/j.apenergy.2020.115614.
[44] Innovation Outlook: Renewable Methanol, IRENA and Methanol Institute, Abu Dhabi, 2021. www.irena.org.
[45] A. Prašnikar, A. Pavlišič, F. Ruiz-Zepeda, J. Kovač, B. Likozar, Mechanisms of copper-based catalyst deactivation during CO2 reduction to methanol, Ind. Eng. Chem. Res. 58 (2019) 13021–13029, https://doi.org/10.1021/acs.iecr.9b01898.
[46] J. Terreni, M. Trottmann, T. Franken, A. Heel, A. Borgschulte, Sorption-enhanced methanol synthesis, Energy Technol. 7 (2019), https://doi.org/10.1002/ente.201801093.
[47] J. van Kampen, J. Boon, F. van Berkel, J. Vente, M. van Sint Annaland, Steam separation enhanced reactions: review and outlook, Chem. Eng. J. 374 (2019) 1286–1303, https://doi.org/10.1016/j.cej.2019.06.031.
[48] R. Freund, O. Zaremba, G. Arnauts, R. Ameloot, G. Skorupskii, M. Dincă, A. Bavykina, J. Gascon, A. Ejsmont, J. Goscianska, M. Kalmutzki, U. Lächelt, E. Ploetz, C.S. Diercks, S. Wuttke, The current status of MOF and COF applications, Angew. Chem. Int. Ed. 60 (2021) 23975–24001, https://doi.org/10.1002/anie.202106259.